Astronomy & Astrophysics

The Northern Cross Fast Radio Burst project

III. The FRB–magnetar connection in a sample of nearby galaxies

D. Pelliciari[1,2], G. Bernardi[1,3,4], M. Pilia[5], G. Naldi[1], G. Pupillo[1], M. Trudu[5,6], A. Addis[7], G. Bianchi[1],
C. Bortolotti[1], D. Dallacasa[1,2], R. Lulli[1], A. Maccaferri[1], A. Magro[8], A. Mattana[1], F. Perini[1], M. Roma[1],
M. Schiaffino[1], G. Setti[1,2], M. Tavani[9,10], F. Verrecchia[11,12], and C. Casentini[9]

[1] INAF-Istituto di Radio Astronomia (IRA), Via Piero Gobetti 101, Bologna, Italy
   e-mail: davide.pelliciari@inaf.it
[2] Dipartimento di Fisica e Astronomia, Universitá di Bologna, Via Gobetti 93/2, 40129 Bologna, Italy
[3] South African Radio Astronomy Observatory, Black River Park, 2 Fir Street, Observatory, Cape Town 7925, South Africa
[4] Department of Physics and Electronics, Rhodes University, PO Box 94, Grahamstown 6140, South Africa
[5] INAF-Osservatorio Astronomico di Cagliari, Via della Scienza 5, 09047 Cuccuru Angius, Selargius CA, Italy
[6] Università degli Studi di Cagliari, Dipartimento di Fisica, S.P. Monserrato-Sestu km 0.7, 09042 Monserrato, CA, Italy
[7] INAF-Osservatorio di Astrofisica e Scienza dello Spazio di Bologna, Via Piero Gobetti 93/3, 40129 Bologna, Italy
[8] Institute of Space Sciences and Astronomy (ISSA) Maths and Physics Building, University of Malta, Msida, MSD 2080, Malta
[9] INAF/IAPS, Via del Fosso del Cavaliere 100, 00133 Roma RM, Italy
[10] Università degli Studi di Roma "Tor Vergata", Via della Ricerca Scientifica 1, 00133 Roma RM, Italy
[11] SSDC/ASI, Via del Politecnico snc, 00133 Roma RM, Italy
[12] INAF-Osservatorio Astronomico di Roma, Via Frascati 33, 00078 Monte Porzio Catone RM, Italy

ABSTRACT

Context. Fast radio bursts (FRBs) are millisecond radio transients observed at cosmological distances. The nature of their progenitors is still a matter of debate, although magnetars are invoked by most models. The proposed FRB–magnetar connection was strengthened by the discovery of an FRB-like event from the Galactic magnetar SGR J1935+2154.
Aims. In this work we aim to investigate how prevalent magnetars such as SGR J1935+2154 are within FRB progenitors.
Methods. To this end, we carried out an FRB search in a sample of seven nearby (<12 Mpc) galaxies with the Northern Cross Radio Telescope for a total of 692 h.
Results. We detected one 1.8 ms burst in the direction of M 101 with a fluence of 58 ± 5 Jy ms. Its dispersion measure of 303 pc cm^{-3} places it most likely beyond M 101. Considering that no significant detection comes indisputably from the selected galaxies, we place a 38 yr^{-1} upper limit on the total burst rate (i.e. including the whole sample) at the 95% confidence level. This upper limit constrains the event rate per magnetar to $\lambda_{\mathrm{mag}} < 0.42$ magnetar^{-1} yr^{-1} or, if combined with literature observations of a similar sample of nearby galaxies, it yields a joint constraint of $\lambda_{\mathrm{mag}} < 0.25$ magnetar^{-1} yr^{-1}. We also provide the first constraints on the expected rate of FRBs hypothetically originating from ultra-luminous X-ray (ULX) sources, since some of the galaxies observed during our observational campaign host confirmed ULXs. We obtain <13 yr^{-1} per ULX for the total sample of galaxies observed.
Conclusions. Our results indicate that bursts with energies $E > 10^{34}$ erg from magnetars such as SGR J1935+2154 appear more rarely compared to previous observations and further disfavour them as unique progenitors for the cosmological FRB population. This provides support to the idea that there is a greater contribution from a population of more exotic magnetars not born via core-collapsed supernovae.

Key words. Local Group – methods: observational – stars: magnetars

1. Introduction

Fast radio bursts (FRBs) are millisecond-long, highly dispersed radio signals with exceptionally high brightness temperatures (10^{32}–10^{35} K) of extragalactic origin (Thornton et al. 2013; Cordes & Chatterjee 2019; Petroff et al. 2019, 2022; Pilia 2021). Since their discovery (Lorimer et al. 2007), about 600 distinct FRB sources have been observed (CHIME/FRB Collaboration 2021), with a host galaxy association for about 25 of them (Tendulkar et al. 2017; Bannister et al. 2019; Ravi et al. 2019, 2022, 2023; Prochaska et al. 2019; Macquart et al. 2020; Marcote et al. 2020; Bhardwaj et al. 2021b; Niu et al. 2022; Nimmo et al. 2022; Ryder et al. 2022; Bhandari et al. 2023;

Driessen et al. 2023; Sharma et al. 2023). Moreover, 50 FRBs were found to be repeating (CHIME/FRB Collaboration 2023), with recent statistical evidence indicating that repeaters may represent a distinct class of sources (Hashimoto et al. 2020; Pleunis et al. 2021; Zhong et al. 2022; Guo & Wei 2022; CHIME/FRB Collaboration 2023). Up to now, only two repeaters, FRB 20180916B and FRB 20121102, have shown periodic activity, with periods of ~16.33 ± 0.12 (Pleunis et al. 2021) and ~161 ± 5 days (Cruces et al. 2021), respectively.

Of the progenitor candidates, magnetars – neutron stars (NSs) powered by the decay of their strong (10^{14}–10^{16} G) magnetic field (Duncan & Thompson 1992; Rea & Esposito 2011; Turolla et al. 2015; Kaspi & Beloborodov 2017) – are the most

Table 1. Properties of the observed NG sample.

	RA (J2000)	Dec (J2000)	D (Mpc)	SFR ($M_\odot$ yr^{-1})	DM$_{\rm ISM}$ (pc cm^{-3})	T (h)
M 31	00$^{\rm h}$42$^{\rm m}$44.3$^{\rm s}$	+41°16′07.5″	0.79 ± 0.03 [1]	0.35 [8]	142	51
IC 342	03$^{\rm h}$46$^{\rm m}$48.5$^{\rm s}$	+68°05′46.0″	3.3 ± 0.3 [2]	2.8 [9]	178	102
M 82	09$^{\rm h}$55$^{\rm m}$52.4$^{\rm s}$	+69°40′46.9″	3.53 ± 0.04 [3]	13 [10]	41.2	184
M 101	14$^{\rm h}$03$^{\rm m}$12.6$^{\rm s}$	+54°20′55.5″	6.4 ± 0.5 [4]	2.9 [11]	30.9	96
NGC 6946	20$^{\rm h}$34$^{\rm m}$52.3$^{\rm s}$	+60°09′13.2″	7.7 ± 0.3 [5]	4.3 [11]	145.8	115
M 106	12$^{\rm h}$18$^{\rm m}$57.6$^{\rm s}$	+47°18′13.4″	7.8 ± 0.6 [6]	2.8 [11]	25.8	84
M 66	11$^{\rm h}$20$^{\rm m}$15.0$^{\rm s}$	+12°59′28.6″	11.1 ± 0.4 [7]	2.7 [11]	31.1	63

Notes. Columns list: coordinates, distances (D), SFRs, the dispersion measure contribution from the MW interstellar medium (DM$_{\rm ISM}$) computed as the maximum between the YM16 (Yao et al. 2017) and NE2001 (Cordes & Lazio 2002, 2003) models, and the total exposure time spent on source. SFRs are estimated from Hα luminosities for all the galaxies but M 82 and IC 342, for which infrared luminosities were used.
References. References for distances are: [1] McConnachie et al. (2005); [2] Karachentsev et al. (2004); [3] Dalcanton et al. (2009); [4] Shappee & Stanek (2011); [5] Anand et al. (2018); [6] Newman et al. (2001); and [7] Hoyt et al. (2019). References for SFRs are: [8] Rahmani et al. (2016); [9] Gao & Solomon (2004); [10] Förster Schreiber et al. (2003); [11] Kennicutt et al. (2008).

widely considered. The FRB–magnetar connection was strengthened by the detection of FRB 20200428, the first Galactic FRB-like event discovered (CHIME/FRB Collaboration 2020; Bochenek et al. 2020); it was observed simultaneously with an X-ray burst (Mereghetti et al. 2020; Ridnaia et al. 2020; Li et al. 2021; Tavani et al. 2021), emitted by the soft gamma repeater J1935+2154 (SGR1935 – hereafter), one of the most active known magnetars (Stamatikos et al. 2014; Lien et al. 2014; Cummings 2014; Kozlova et al. 2016; Younes et al. 2017). The reported isotropic-equivalent energy emitted at radio wavelengths by this burst, $E_{\rm SGR} \simeq 2 \times 10^{34}$ erg (Bochenek et al. 2020; Margalit et al. 2020), lies between those of the energetic pulsar giant radio pulses (see e.g., Kuzmin 2007) and extragalactic FRBs. Further observations revealed fainter bursts from SGR1935 (Zhang et al. 2020; Burgay et al. 2020; Good & CHIME/FRB Collaboration 2020; Alexander & Fedorova 2020; Kirsten et al. 2021; Dong & CHIME/FRB Collaboration 2022; Maan et al. 2022; Huang et al. 2022; Pearlman & CHIME/FRB Collaboration 2022).

Since magnetars are connected to a young stellar population, they are expected to be found in regions of star formation. While this has been observed for some FRBs (Chatterjee et al. 2017; Marcote et al. 2017, 2020; Bassa et al. 2017; Tendulkar et al. 2017, 2021; Ravi et al. 2019; Bhardwaj et al. 2021b; Piro et al. 2021; Niu et al. 2022; Nimmo et al. 2022), others have been found in galaxies with low star formation rates (SFRs), mainly in their outskirts (Heintz et al. 2020; Mannings et al. 2021; Bhandari et al. 2022). Notably, the repeating FRB 20200120E was recently found in a globular cluster in the nearby galaxy (NG) M 81 (Kirsten et al. 2022). It is also theoretically possible to find young magnetised NSs in globular clusters, formed either via the accretion-induced collapse of a white dwarf (WD; Tauris et al. 2013; Wang & Liu 2020) or the collapse of a compact binary system induced by a WD-WD, WD-NS or NS-NS merger (Giacomazzo & Perna 2013; Schwab et al. 2016; Zhong & Dai 2020).

CHIME/FRB Collaboration (2020) observed a sample of 15 NGs within 12 Mpc with SFRs higher than that of the Milky Way (MW) in order to search for SGR1935-like FRBs– (i.e. bursts with energy $E_0 > 4 \times 10^{34}$ erg). The advantage of targeting NGs over the MW is that the whole population of magnetars is simultaneously observed, therefore increasing the probability of detecting a burst with respect to individual magnetars. No bursts were observed, allowing them to place a con-

straint on the burst rate of SGR1935-like events $0.007 < \lambda_{\rm mag} < 0.4$ yr^{-1} magnetar^{-1}, where the lower limit is set by the detection of the SGR1935 burst itself (CHIME/FRB Collaboration 2020).

In this work we present long monitoring observations of a sample of NGs taken with the Northern Cross (NC) Radio Telescope in the search for FRBs with the aim to study the FRB–magnetar connection, following CHIME/FRB Collaboration (2020). We note that some of the galaxies observed within our observational campaign host confirmed ultra–luminous X-ray (ULX) sources, accreting binary systems with X-ray luminosities $L_{\rm X} \geq 10^{39}$ erg s^{-1}, which is significantly higher than any X-ray luminosity emitted by stellar processes (Fabbiano 1989; Kaaret et al. 2017).

The paper is structured as follows: Sect. 2.1 describes the observations and the sample of NGs observed, Sect. 3 presents constraints on the FRB burst rate of magnetars (Sect. 3.1) and ULXs (Sect. 3.2) determined using these observations. Finally, the implications that our constraints have on the connection between FRBs and their progenitors, along with our conclusions, are discussed in Sect. 4.

2. An FRB search in a sample of nearby galaxies

2.1. Sample description and observations

Our sample consists of seven galaxies within a maximum distance of 12 Mpc, whose characteristics are summarized in Table 1. We selected them based on their reported high SFRs, since magnetars such as SGR1935, born through core-collapse supernovae (CCSNe), trace young star formation sites. Apart from M 31 and IC 342, all the galaxies were already included in the sample observed by CHIME/FRB Collaboration (2020). We included M 31 for its proximity and similarity to the MW. As already mentioned, among the galaxies observed, M 82, M 101, IC 342 and NGC 6946 host confirmed ULXs. They are M 82 X-1 (Ptak & Griffiths 1999), M 101 X-1 (Stetson et al. 1998), IC 342 X-1, IC 342 X-2 (Rana et al. 2015) and NGC 6946 X-1 (Fabbiano & Trinchieri 1987; Roberts & Colbert 2003). These objects are currently believed to be the result of super-Eddington accretion onto a stellar mass black hole (BH; e.g. Liu et al. 2013), or a NS (Pintore et al. 2020, and references therein).

We monitored each galaxy daily during its transit through the telescope's primary beam using eight cylinders of the north-south arm of the array (we refer the reader to Locatelli et al. 2020,
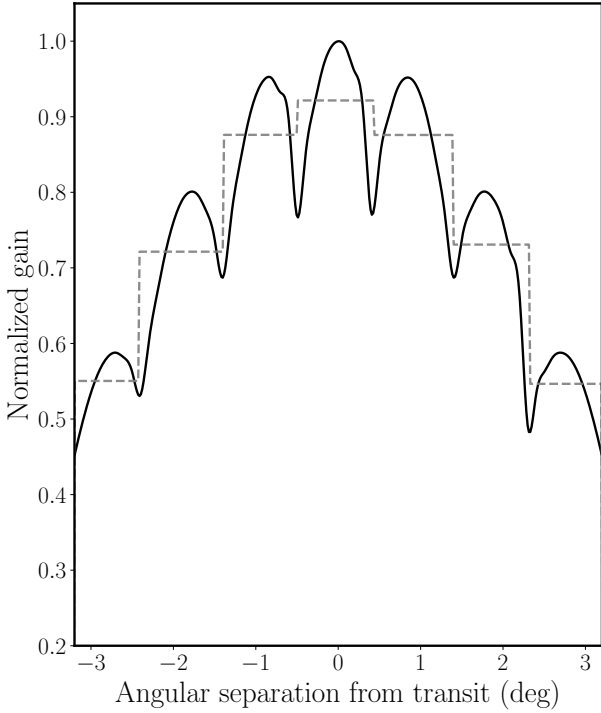
Fig. 1. Normalized NC beam-forming response (solid line) as the source transits across the telescope field of view. Dashed lines represent the average value of the telescope beam response for each delay bin.

for details of the system). Due to limitations of the current acquisition software, a source cannot be tracked continuously as it moves across the telescope's field of view; therefore, we employed the 'shift and track' strategy used in Trudu et al. (2022), where seven discrete delay values are approximately equally spaced in angular size to cover the field of view. The resulting telescope beam pattern is shown in Fig. 1, where the seven peaks corresponding to the seven beam-forming delays are clearly visible. Such a beam pattern implies that the sensitivity to the source varies by up to 40% as it transits through the primary beam. As the variation in the beam response within each delay bin is small ($\approx 10\%$), in the following analysis we assume it to be constant and equal to its average value (dashed line in Fig. 1). The energy detection threshold, $E_{\min}$, for a burst observed in the delay bin j from the galaxy i can be written as

$$E_{\min,i,j} = 4\pi D_i^2 \, \Delta\nu \, \frac{F}{A_j}, \tag{1}$$

where D_i is the source distance, $\Delta\nu = 16$ MHz the observing bandwidth, A_j the average beam gain in the jth delay bin and $F = 38$ Jy ms the NC fluence threshold corresponding to the peak of the central beam assuming a 10σ detection threshold (Trudu et al. 2022). In this work we assume 1 ms as the reference burst duration.

Observations started on December 26, 2021, and ended on August 21, 2022, for a total of 692 h. Data were stored to disk with a time resolution of 138.24 μs and a frequency channel width of 14.468 kHz. We calibrated our data using interferometric observations of Case A (see Locatelli et al. 2020, for details on the calibration procedure), carried out approximately at the beginning, halfway and at the end of the observational campaign. Receiver phases and amplitudes remained fairly constant over week-long timescales; nevertheless, our observing campaign was interspersed with monthly observations of the pul-

sar B0329+54 and the repeating FRB 20180916B (CHIME/FRB Collaboration 2019). Both sources served as calibration tests for the stability of our system and, at the same time, FRB 20180916B was observed within its window of expected activity (CHIME/FRB Collaboration 2019; Pastor-Marazuela et al. 2021; Pleunis et al. 2021; Trudu et al. 2022) for the purpose of obtaining multiwavelength observations (Pilia et al. 2020; Tavani et al. 2020; Trudu et al. 2022).

We regularly detected single pulses from B0329+54 at its nominal dispersion measure (DM), ~26.8 pc cm^{-3} (Hassall et al. 2012), and detected two new bursts from FRB 20180916B, in addition to those presented in Trudu et al. (2022), in agreement with the expected repetition rate.

Figure 2 shows their de-dispersed waterfall plots, labelled B4 and B5 to follow the Trudu et al. (2022) nomenclature, and their best-fit values are listed in Table 2. These detections provide evidence for calibration stability across the whole campaign.

The search for FRBs in our galaxy sample was performed using the SPANDAK pipeline (Gajjar et al. 2018), which flags radio frequency interference (RFI) through RFIFIND (Ransom et al. 2002) and searches for single pulses with HEIMDALL (Barsdell et al. 2012). We used the same search setup described in Trudu et al. (2022), within the $0 < DM < 1000$ pc cm^{-3} range, with a signal-to-noise ratio (S/N) greater than six and a boxcar duration shorter than 35 ms in order to balance the search time and our scientific goals whilst remaining consistent with the observed width distribution of FRBs (CHIME/FRB Collaboration 2021; Petroff et al. 2022).

2.2. FRB detection from the direction of M 101

We found no candidates with a $S/N > 10$ throughout the whole campaign and ~100 candidates with $6 \le S/N \le 10$ that were further visually inspected and double-checked. Most candidates were discarded due to the presence of RFI contamination and noise properties that showed deviations from a theoretical Gaussian distribution. The only candidate that conservatively passed the selection, detected with a $S/N \sim 11$, is shown in Fig. 3.

We assessed the likelihood of a candidate signal by computing the number of false candidates with S/N higher than the detection threshold, expected because of noise outliers. The number of false positive events is a function of the S/N and can be computed as (Cordes & McLaughlin 2003)

$$N_{\text{false}}(>S/N) = 2 \, N_{\text{DM}} \, \frac{\Delta T}{\mathrm{d}t} \, P(>S/N), \tag{2}$$

where N_{DM} is the number of DM trials considered in the FRB search, set internally in HEIMDALL, ΔT the total duration of the observations, dt the time sample duration, and

$$P(>S/N) = \frac{2}{\sqrt{\pi}} \int_0^x e^{-z^2} \mathrm{d}z \equiv \frac{1}{2} \left[1 - \mathrm{erf}\left(\frac{S/N}{\sqrt{2}}\right) \right] \tag{3}$$

the probability that an event is due to a noise statistical fluctuation. In our case, $N_{\text{DM}} \sim 3000$, $\Delta T = 692$ h, and d$t \sim 138$ μs, resulting in $N_{\text{false}} \sim 10^{-9}$ for $S/N \ge 10$. Hence, we consider our candidate to be a genuine FRB.

The burst, hereafter FRB 20220320, was detected on 2022 March 30 UT = 01:14:02.40 (Barycentric time of arrival, ∞ MHz), in the direction of M 101, and its properties are listed in Table 3.

We measured a DM = 303 ± 2 pc cm^{-3}, which disfavours a local origin. The DM contribution along the line of sight of M 101 due to the interstellar medium (ISM) is DM$_{\text{ISM}} \simeq 23$–31 pc cm^{-3},
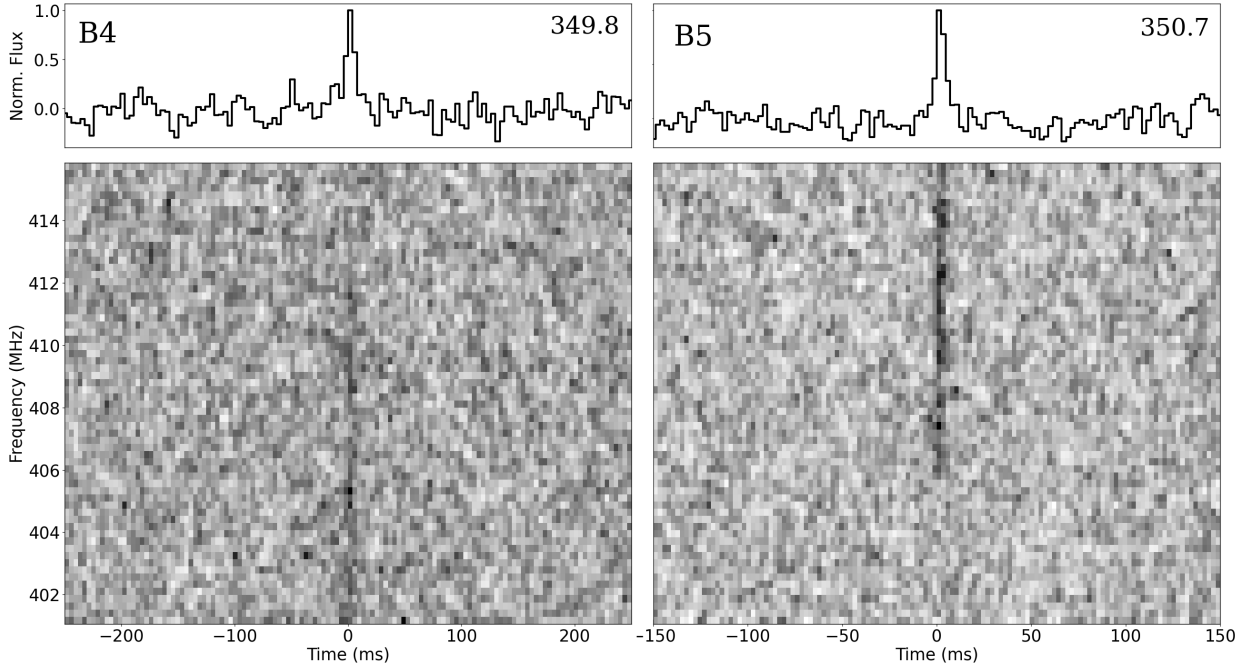
Fig. 2. Bursts from FRB 20180916B observed on April 30th 2022 (left panel) and August 9th 2022 (right panel), respectively. Bottom panels show the dynamic spectra, while the top panels show the frequency averaged profiles. The best-fit DMs (in pc cm^{-3}) at which the bursts were de-dispersed are reported in the top right corner of each plot. Data were down-sampled to have 64 frequency channels, each 0.25 MHz wide, and time bins with 2.2 ms width for better display.

Table 2. Properties of B4 and B5 bursts from FRB 20180916B.

Parameter	B4	B5
TOA (MJD)	59699.52603591	59800.25184782
S/N	15	20
DM (pc cm^{-3})	349.8 ± 0.1	350.7 ± 0.1
Δt (ms)	6.35 ± 0.1	5.7 ± 0.3
Flux density (Jy)	15 ± 1	19 ± 1
Fluence (Jy ms)	96 ± 6	108 ± 5

Notes. We report, from the top row to the bottom, the barycentric time of arrival (TOA) expressed as the modified julian day (MJD), the signal to noise ratio (S/N), the fit-optimized DM, the full width at half maximum (FWHM) duration, the flux density and the fluence of the bursts.

according to the NE2001 (Cordes & Lazio 2002, 2003) and the YMW16 (Yao et al. 2017) electron density models, while the contribution from the Galactic halo is ~50 pc cm^{-3} (Agarwal et al. 2019; Macquart et al. 2020; Yamasaki & Totani 2020; Lemos et al. 2023). Finally, the intergalactic medium (considering $z \simeq 0.001$) contributes approximately ~2 pc cm^{-3} (Macquart et al. 2020), although this value, for low redshift galaxies, depends on the line of sight (Li et al. 2019). These contributions, if coming from M 101, would imply a moderately high DM$_{\rm host}$, $\simeq$220 pc cm^{-3}. In our case, the almost face-on inclination of M 101 seems to disfavour a large DM$_{\rm host}$ for M 101 (Xu & Han 2015). Although James et al. (2022), by analysing 16 FRBs from Australian Square Kilometre Array Pathfinder (ASKAP) observations, found $\langle$DM$_{\rm host}\rangle \sim 186 \pm 50$ pc cm^{-3}, which would be compatible with an origin from M 101, other works point towards lower values for the host DM contribution (Niino 2020; Zhang et al. 2020). This is further evidence that an association with M 101 is unlikely.

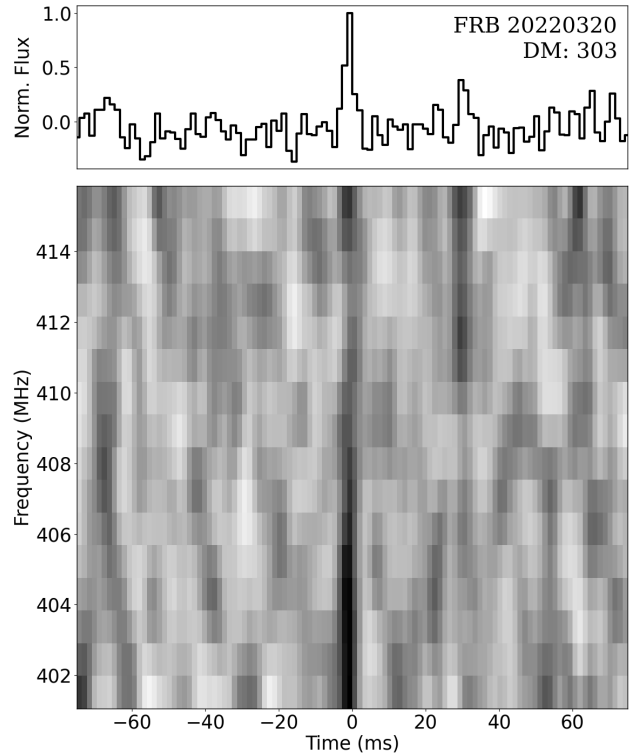**Fig. 3.** De-dispersed profile of FRB 20220320. The top panel shows the frequency-averaged time series, and the bottom panel shows its dynamic spectrum, coherently de-dispersed at DM = 303 pc cm^{-3}.

If we consider the burst to be originating farther away, assuming a more conservative value DM$_{\rm host} \simeq 100$ pc cm^{-3}, the burst would be placed at a maximum redshift of $z \sim 0.18$,

Table 3. Observational properties of FRB 20220320.

Parameter	Value
RA (J2000, deg)	211 (3)
Dec (J2000, deg)	54.4 (5)
TOA	2022-03-20 01:14:02.40 (UT)
S/N	11
DM (pc cm^{-3})	303 ± 2
Δt (ms)	1.8 ± 0.3
Flux density (Jy)	32 ± 3
Fluence (Jy ms)	58 ± 5

Notes. The uncertainty on the FRB position corresponds to the beam full width at half maximum.

that is to say, at a luminosity distance of ∼870 Mpc. For the distance estimation we considered a seven-year Wilkinson Microwave Anisotropy Probe (WMAP7) cosmology (Komatsu et al. 2011) to be consistent with Macquart et al. (2020). Given this maximum redshift, its spectral luminosity would be at most 6.3×10^{33} erg s^{-1} Hz^{-1}, well within the range of extragalactic FRB spectral luminosities (Bochenek et al. 2020; CHIME/FRB Collaboration 2020; Luo et al. 2020).

3. Upper limits on the FRB repetition rate from our observations

In this section we show how the observations conducted in our NG campaign allowed us to extract important upper limits on the FRB burst rate. In particular, we developed a simple model to calculate the expected rate of FRB events from the whole sample of galaxies listed in Table 1, considering as a first case a single population of SGR1935-like magnetars as FRB progenitors. By taking λ_{mag}, the average burst rate per magnetar, and γ, the power-law energy distribution slope for magnetar bursts, as free parameters, we discuss how the upper limits on the rate from the whole galaxy sample translate into upper limits on λ_{mag} and γ. We also discuss how our observations coul constrain the FRB event rate if FRBs originated from ULXs. Indeed, accretion-based mechanisms for the FRB engine have been proposed (Waxman 2017; Katz 2017, 2020; Sridhar et al. 2021; Deng et al. 2021).

3.1. SGR1935-like magnetars

We started by computing the total burst rate from our galaxy sample, considering a single population of magnetars similar to SGR1935. This means that we restricted our analysis to magnetars that have radio efficiencies $\eta \sim 10^{-5}$, the ratio of energy radiated in the radio and X-ray bands by SGR1935 (Mereghetti et al. 2020; Ridnaia et al. 2020; CHIME/FRB Collaboration 2020; Bochenek et al. 2020; Tavani et al. 2021), and burst energetics $E \geq E_0$, where $E_0 = 2 \times 10^{34}$ erg is the isotropic radio energy released by FRB 20200428 (Bochenek et al. 2020; Margalit et al. 2020; CHIME/FRB Collaboration 2020). This energy follows by considering $d = 7$ kpc to be the distance to SGR1935 (Margalit et al. 2020).

Following CHIME/FRB Collaboration (2020), we assumed that the magnetar burst rate $\mathcal{R}$ from a given galaxy is proportional to its SFR. We computed the number of SGR1935-like magnetars residing in a certain galaxy by scaling for $N_{\mathrm{mag}}/\mathrm{SFR}_{\mathrm{MW}}$, with $N_{\mathrm{mag}} = 29$ (Olausen & Kaspi 2014; Kaspi & Beloborodov

2017) the number of Galactic magnetars and $\mathrm{SFR}_{\mathrm{MW}} = 1.65 \pm 0.19 \, M_\odot \, \mathrm{yr}^{-1}$ the Galactic SFR (Licquia & Newman 2015).

With these prescriptions, the rate expected from the galaxy i of our sample can be expressed as

$$\mathcal{R}(\lambda_{\mathrm{mag}}, \gamma; > E_{\mathrm{min},i,j}) = N_{\mathrm{mag}} \frac{\mathrm{SFR}_i}{\mathrm{SFR}_{\mathrm{MW}}}$$
$$\times \int_{E_{\mathrm{min},i,j}}^{E_{\mathrm{max}}} K_0 \left(\frac{E}{E_0} \right)^{-\gamma} \Theta[E - E_0] \, \mathrm{d}E, \tag{4}$$

where $E_{\mathrm{min},i,j}$ is the minimum burst energy detectable from the galaxy i in the delay bin j (Eq. (1)). The integral is the burst rate energy function, which we assumed to follow a power law with index γ. We note that the Heaviside function, Θ, restricts the case to SGR1935-like bursts (i.e. with energy $E \geq E_0$). We considered the maximum energy, E_{max}, to be

$$E_{\mathrm{max}} = \eta E_{\mathrm{mag}}, \tag{5}$$

with $\eta \sim 10^{-5}$ and E_{mag} the total magnetic energy reservoir for a magnetar with magnetic field B (Margalit et al. 2020):

$$E_{\mathrm{mag}} = 3 \times 10^{49} \left(\frac{B}{10^{16} \, \mathrm{G}} \right)^2 \mathrm{erg}. \tag{6}$$

We considered $B = 2 \times 10^{14}$ G, the magnetic field strength of SGR1935 (Israel et al. 2016), and verified that a higher value for B does not appreciably affect our results.

The burst rate normalization, K_0, can be expressed as a function of the burst rate per magnetar λ_{mag}:

$$\lambda_{\mathrm{mag}} = \int_{E_0}^{E_{\mathrm{max}}} K_0 \left(\frac{E}{E_0} \right)^{-\gamma} \mathrm{d}E, \tag{7}$$

yielding:

$$K_0 = \lambda_{\mathrm{mag}} \frac{(1 - \gamma) E_0^{-\gamma}}{E_{\mathrm{max}}^{-\gamma+1} - E_0^{-\gamma+1}}. \tag{8}$$

Equation (4) can therefore be re-written as

$$\mathcal{R}(\lambda_{\mathrm{mag}}, \gamma; > E_{\mathrm{min},i,j}) = N_{\mathrm{mag}} \lambda_{\mathrm{mag}} \frac{\mathrm{SFR}_i}{\mathrm{SFR}_{\mathrm{MW}}} \frac{E_{\mathrm{max}}^{-\gamma+1} - E_{\mathrm{min},i,j}^{-\gamma+1}}{E_{\mathrm{max}}^{-\gamma+1} - E_0^{-\gamma+1}}. \tag{9}$$

We could then compute the total expected burst rate from our NG sample as the sum of the rate for each galaxy in each delay bin, weighted by their corresponding integration time:

$$\mathcal{R}_{\mathrm{tot}}(\lambda_{\mathrm{mag}}, \gamma) = \frac{\sum_i^N \sum_j^{N_\mathrm{b}} \mathcal{R}(\lambda_{\mathrm{mag}}, \gamma; > E_{\mathrm{min},i,j}) \, T_{i,j}}{\sum_i^N \sum_j^{N_\mathrm{b}} T_{i,j}}, \tag{10}$$

where $N_\mathrm{b} = 7$ is the number of delay bins and $T_{i,j}$ is the total integration time of the ith galaxy in the delay bin j. The total expected burst rate is mildly dependent upon the slope of the energy distribution and much more significantly dependent upon the burst rate per magnetar as can be visually assessed in Fig. 4. Our observations led to a 95% confidence level (CL; Gehrels 1986) upper limit on the total burst rate of $\mathcal{R}_{\mathrm{tot}} < 38 \, \mathrm{yr}^{-1}$. By imposing this upper limit, we obtain a 95% CL constraint on the burst rate per magnetar that varies between $\lambda_{\mathrm{mag}} < 0.38 \, \mathrm{magnetar}^{-1} \, \mathrm{yr}^{-1}$ for $\gamma \leq 1$ and $\lambda_{\mathrm{mag}} < 0.47 \, \mathrm{magnetar}^{-1} \, \mathrm{yr}^{-1}$ for $\gamma \simeq 3$. After marginalizing over the energy distribution slope γ, we derive $\lambda_{\mathrm{mag}} < 0.42 \, \mathrm{magnetar}^{-1} \, \mathrm{yr}^{-1}$.
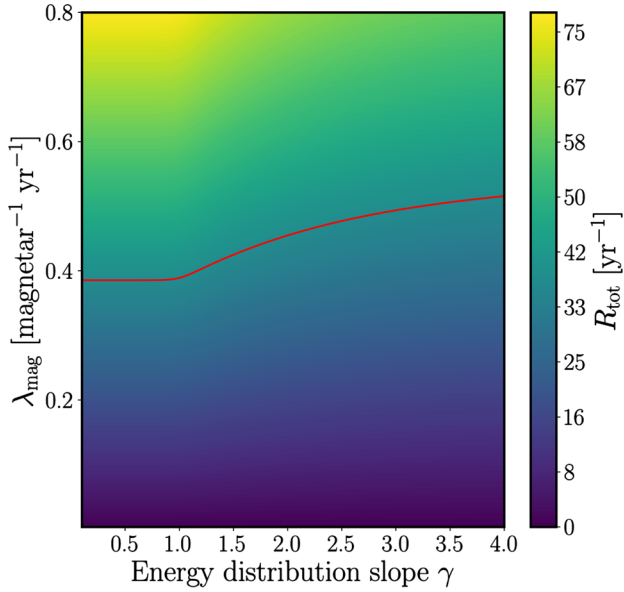
Fig. 4. Expected burst rate (colour-map) as a function of the energy distribution slope, γ, and the SGR1935-like burst rate per magnetar, λ_{mag}, from the whole observing campaign of NGs. The red line is the 95% CL upper limit obtained via our observations.

Previous works derived constraints for the magnetar burst rate. In particular, CHIME/FRB Collaboration (2020) obtained $0.007 < \lambda_{\mathrm{mag}} < 0.4\,\mathrm{magnetar}^{-1}\,\mathrm{yr}^{-1}$ at the 95% CL from the detection of FRB 20200428 and the non-detection from a sample of 15 NGs. However, the authors adopted slightly different values than us for the distances and SFRs of the galaxies that are common to our sample (see their Extended Data Table 1), and they considered a lower $\mathrm{SFR_{MW}}$ of $1\,M_{\odot}\,\mathrm{yr}^{-1}$. If we use their values in our estimate, we obtain $\lambda_{\mathrm{mag}} < 0.3\,\mathrm{magnetar}^{-1}\,\mathrm{yr}^{-1}$. By combining our observations with CHIME/FRB Collaboration (2020), we can obtain an even further improved upper limit on λ_{mag}. Assuming the distance and SFR values presented in Table 1 for both samples, we recomputed the total rate expected from the joint observations (Eqs. (9) and (10)), which has to be compared with the upper limit obtained from the total observing time (~1370 h). As a result, we obtain $\lambda_{\mathrm{mag}} < 0.25\,\mathrm{magnetar}^{-1}\,\mathrm{yr}^{-1}$ at the 95% CL, the most stringent upper limit on the burst rate per magnetar to date. In Sect. 4 we discuss this result in the framework of the FRB–magnetar connection.

3.2. Ultra-luminous X-ray sources

An alternative formation channel to the more standard magnetar models predicts that FRBs can be produced by short-lived relativistic flares from super-Eddington accreting NSs and BHs (Sridhar et al. 2021). The isotropic energy emitted by this kind of FRB is postulated to lie in the range $10^{34}\,\mathrm{erg}$–$10^{45}\,\mathrm{erg}$ (Sridhar et al. 2021), which implies that these sources would have been detected with the NC sensitivity. Therefore, the observing time spent on these galaxies is useful for placing an upper limit on the rate of FRBs produced by these accreting objects.

We followed the approach described in Sect. 3 and expressed the rate expected from the population of ULXs, $\mathcal{R}_{u,i}$, in the galaxy i of our sample:

$$\mathcal{R}_{u,i}(\lambda_u) = N_{u,i}\,\lambda_u, \tag{11}$$

where $N_{u,i}$ is the number of ULX sources expected in the galaxy i and λ_u is the average burst rate per ULX for energies in the

Table 4. Upper limits for the FRB repetition rate (last column) coming from confirmed ULXs.

ULX	N_u	λ_u (yr^{-1})
IC 342 X-1, IC 342 X-2	2	<128
M 82 X-2	1	<140
M 101 X-1	1	<273
NGC 6946 X-1	1	<227
All	14	<13

Notes. In the second column we report the number of ULXs present in a given galaxy. The last row considers the total expected ULX ensemble derived from Eq. (12).

$10^{34} < E < 10^{45}$ erg range. The number of ULX sources can be expressed as a function of the SFR (Kovlakas et al. 2020):

$$N_{u,i} = 0.51\,\frac{\mathrm{SFR}_i}{M_{\odot}\,\mathrm{yr}^{-1}}. \tag{12}$$

We expect from Eq. (12) a total of ~14 ULXs in the galaxies we observed. The total expected burst rate, $\mathcal{R}_{u,\mathrm{tot}}$, from our NG sample then becomes:

$$\mathcal{R}_{u,\mathrm{tot}}(\lambda_u) = \frac{\sum_i^N \sum_j^{N_b} \mathcal{R}_{u,i}(\lambda_u)\,T_{i,j}}{\sum_i^N \sum_j^{N_b} T_{i,j}}. \tag{13}$$

The observed upper limit at the 95% CL on the total burst rate is $\simeq 38\,\mathrm{yr}^{-1}$, the same as determined in Sect. 3.1, since it depends only on the total observing time. Therefore, by imposing $\mathcal{R}_{u,\mathrm{tot}} < 38\,\mathrm{yr}^{-1}$, we obtain $\lambda_u < 13\,\mathrm{yr}^{-1}$ for the average burst rate per ULX. This is the first upper limit on the FRB repetition rate hypothetically coming from ULXs. We note that this upper limit is two to three orders of magnitude lower than the reported repetition rate of most active repeaters from FRB 20121102A and FRB 20180916B, $r \sim 10^3\,\mathrm{yr}^{-1}$ (Margalit et al. 2020). We also find this contrast by computing the repetition rate for confirmed ULXs only, that is to say, without estimating the population of ULXs from Eq. (12) and only considering already discovered ULXs in the galaxies we observed. We report the upper limits obtained for each case in Table 4 and discuss the possible implications of these results in the following section.

4. Discussion and conclusions

In this paper we present an FRB search in a sample of seven NGs taken with the NC Radio Telescope. The campaign was 692 h long and yielded the detection of a 58 Jy ms, 1.8 ms long burst with a $\mathrm{DM} = 303\,\mathrm{pc\,cm}^{-3}$, observed in the direction of M 101, although most likely coming from a more distant source. Therefore, we consider that no detections came from the monitored galaxies. We used this result to investigate the connection between FRBs and magnetars, by computing the total burst rate, $\mathcal{R}_{\mathrm{tot}}$, expected from our galaxy sample, assuming, as unique FRB progenitors, magnetars such as SGR J1935+2154, and obtaining $\mathcal{R}_{\mathrm{tot}} < 38\,\mathrm{yr}^{-1}$ at the 95% CL. We considered λ_{mag}, the average burst rate per magnetar, and γ, the slope of the burst energy distribution, as free parameters for our SFR-based model. In addition, we derived the average FRB rate per ULX from the same observations of NGs. Among the target galaxies of our observational campaign, some host confirmed ULXs, from which, at least theoretically, an FRB would have obtained enough energy (Sridhar et al. 2021) to be detected by the NC.

Since the detection of the Galactic FRB-like signal, it has been tempting to claim that magnetars such as SGR1935 (i.e. magnetars similar in energetics and formed through CCSNe) represent the entire cosmological population of FRBs. Although the implied volumetric rate from the detection of FRB 20200428 is consistent with the faint energy of the cosmological rate density (Lu et al. 2022), SGR1935-like magnetars cannot explain the high repetition rate of active repeaters (Margalit et al. 2020). Moreover, FRB 20200428 is about one order of magnitude fainter than the average FRB (Bochenek et al. 2020; CHIME/FRB Collaboration 2020; Luo et al. 2020), although giant magnetar flares may be bright enough to fill the gap (Margalit et al. 2020). The discrepancy in the repetition rate, along with the discovery of the M81 repeater localized in a globular cluster (Bhardwaj et al. 2021b; Kirsten et al. 2021), led to consider other, more exotic NS formation channels (Kremer et al. 2021, 2023), and question the presence of a single population of magnetars as FRB progenitors.

Our observations do not constrain the burst energy slope well, although they somewhat disfavour flat slopes ($\gamma < 1$) over steeper ones ($\gamma > 1$). The average burst rate per magnetar is, instead, constrained to be $\lambda_{\mathrm{mag}} < 0.42\,\mathrm{magnetar}^{-1}\,\mathrm{yr}^{-1}$. This upper limit halves the range for the magnetar burst rate implied by the detection from the Survey for Transient Astronomical Radio Emission 2 (STARE2; Bochenek et al. 2020), $0.0036 < \lambda_{\mathrm{mag}} < 0.8\,\mathrm{magnetar}^{-1}\,\mathrm{yr}^{-1}$, consistently with the results from Canadian Hydrogen Intensity Mapping Experiment's (CHIME) NG observations, $0.007 < \lambda_{\mathrm{mag}} < 0.4\,\mathrm{magnetar}^{-1}\,\mathrm{yr}^{-1}$ (CHIME/FRB Collaboration 2020). We also show how the upper limit lowers to $\lambda_{\mathrm{mag}} < 0.25\,\mathrm{magnetar}^{-1}\,\mathrm{yr}^{-1}$ if we consider our NG observations combined with the monitoring reported in CHIME/FRB Collaboration (2020).

Considering the STARE2 detection, Margalit et al. (2020) already pointed out that the cosmological FRB rate, including repeating sources, can be explained only by adding a second magnetar population that is younger and with a stronger magnetic field with respect to the SGR1935-like ones (Margalit et al. 2019; Blanchard et al. 2016). This second population includes more exotic magnetars, not born through the usual supernova core collapse, but through a much rarer formation channel. Our constraints imply that the burst rate per magnetar of SGR-like events is approximately a factor of two smaller than previously reported, implying rarer events. From the perspective of a two-population model, our results imply that rare magnetars should be more prominent than considered earlier in order to compensate for the smaller burst rate from SGR1935-like magnetars. Moreover, the detection of FRB 20200120E in a globular cluster (Bhardwaj et al. 2021a; Kirsten et al. 2022) has similar implications (Lu et al. 2022), namely that the formation of magnetars is possible inside globular clusters through compact object mergers, accretion-induced collapse, or a WD-merger-induced collapse (Kirsten et al. 2022; Kremer et al. 2021, 2023). However, the nanosecond structures observed in some bursts from FRB 20200120E could be explained in terms of a recycled millisecond pulsar origin (Majid et al. 2021; Kremer et al. 2021). Hence, it is not clear whether M81-like FRBs could represent this needed population of rarer FRB progenitors.

Among other exotic but prominent progenitor models, we find accretion-based mechanisms (Waxman 2017; Katz 2017, 2020; Sridhar et al. 2021; Deng et al. 2021). In particular, the recent model of Sridhar et al. (2021) is able to explain both the energetics and the chromaticity behaviour seen in FRB 20180916B (Pastor-Marazuela et al. 2021). Estimating the total number of ULXs present in our sample of galaxies to be 14,

we have constrained the average rate of FRB events per ULX to $\lambda_u < 13\,\mathrm{yr}^{-1}$ at the 95% CL. We have also provided individual upper limits for each monitored ULX. These initial estimates show a discrepancy of a few orders of magnitude when compared to the repetition rates of the most active repeaters (Margalit et al. 2020). As already pointed by Sridhar et al. (2021), a strongly magnetised object in the compact pair could be necessary to power cosmological FRB luminosities, making these events much rarer and more difficult to detect. In conclusion, our limits on the burst rate disfavour both magnetars and ULXs as progenitors of very active repeating sources such as FRB 20180916B and FRB 20121102A.

References

Agarwal, D., Lorimer, D. R., Fialkov, A., et al. 2019, MNRAS, 490, 1
Alexander, R., & Fedorova, V. 2020, ATel, 14186, 1
Anand, G. S., Rizzi, L., & Tully, R. B. 2018, AJ, 156, 105
Bannister, K. W., Deller, A. T., Phillips, C., et al. 2019, Science, 365, 565
Barsdell, B. R., Bailes, M., Barnes, D. G., & Fluke, C. J. 2012, MNRAS, 422, 379
Bassa, C. G., Tendulkar, S. P., Adams, E. A. K., et al. 2017, ApJ, 843, L8
Bhandari, S., Heintz, K. E., Aggarwal, K., et al. 2022, AJ, 163, 69
Bhandari, S., Gordon, A. C., Scott, D. R., et al. 2023, ApJ, 948, 67
Bhardwaj, M., Gaensler, B. M., Kaspi, V. M., et al. 2021a, ApJ, 910, L18
Bhardwaj, M., Kirichenko, A. Y., Michilli, D., et al. 2021b, ApJ, 919, L24
Blanchard, P. K., Berger, E., & Fong, W.-F. 2016, ApJ, 817, 144
Bochenek, C. D., Ravi, V., Belov, K. V., et al. 2020, Nature, 587, 59
Burgay, M., Pilia, M., Bernardi, G., et al. 2020, ATel, 13783, 1
Chatterjee, S., Law, C. J., Wharton, R. S., et al. 2017, Nature, 541, 58
CHIME/FRB Collaboration (Andersen, B. C., et al.) 2019, ApJ, 885, L24
CHIME/FRB Collaboration (Andersen, B. C., et al.) 2020, Nature, 587, 54
CHIME/FRB Collaboration (Amiri, M., et al.) 2021, ApJS, 257, 59
CHIME/FRB Collaboration (Andersen, B. C., et al.) 2023, ApJ, 947, 83
Cordes, J. M., & Chatterjee, S. 2019, ARA&A, 57, 417
Cordes, J. M., & Lazio, T. J. W. 2002, arXiv e-prints [arXiv:astro-ph/0207156]
Cordes, J. M., & Lazio, T. J. W. 2003, arXiv e-prints [arXiv:astro-ph/0301598]
Cordes, J. M., & McLaughlin, M. A. 2003, ApJ, 596, 1142
Cruces, M., Spitler, L. G., Scholz, P., et al. 2021, MNRAS, 500, 448
Cummings, J. R. 2014, GRB Coordinates Network, 16530, 1
Dalcanton, J. J., Williams, B. F., Seth, A. C., et al. 2009, ApJS, 183, 67
Deng, C.-M., Zhong, S.-Q., & Dai, Z.-G. 2021, ApJ, 922, 98
Dong, F. A., & CHIME/FRB Collaboration 2022, ATel, 15681, 1
Driessen, L. N., Barr, E., Buckley, D., et al. 2023, MNRAS, submitted [arXiv:2302.09787]
Duncan, R. C., & Thompson, C. 1992, ApJ, 392, L9
Fabbiano, G. 1989, ARA&A, 27, 87
Fabbiano, G., & Trinchieri, G. 1987, ApJ, 315, 46
Förster Schreiber, N. M., Genzel, R., Lutz, D., & Sternberg, A. 2003, ApJ, 599, 193
Gajjar, V., Siemion, A. P. V., Price, D. C., et al. 2018, ApJ, 863, 2
Gao, Y., & Solomon, P. M. 2004, ApJ, 606, 271
Gehrels, N. 1986, ApJ, 303, 336
Giacomazzo, B., & Perna, R. 2013, ApJ, 771, L26
Good, D., & CHIME/FRB Collaboration 2020, ATel, 14074, 1
Guo, H.-Y., & Wei, H. 2022, JCAP, 2022, 010
Hashimoto, T., Goto, T., On, A. Y. L., et al. 2020, MNRAS, 498, 3927
Hassall, T. E., Stappers, B. W., Hessels, J. W. T., et al. 2012, A&A, 543, A66
Heintz, K. E., Prochaska, J. X., Simha, S., et al. 2020, ApJ, 903, 152
Hoyt, T. J., Freedman, W. L., Madore, B. F., et al. 2019, ApJ, 882, 150
Huang, Y. X., Xu, H., Xu, Y. H., et al. 2022, ATel, 15707, 1
Israel, G. L., Esposito, P., Rea, N., et al. 2016, MNRAS, 457, 3448
James, C. W., Ghosh, E. M., Prochaska, J. X., et al. 2022, MNRAS, 516, 4862
Kaaret, P., Feng, H., & Roberts, T. P. 2017, ARA&A, 55, 303
Karachentsev, I. D., Karachentseva, V. E., Huchtmeier, W. K., & Makarov, D. I. 2004, AJ, 127, 2031
Kaspi, V. M., & Beloborodov, A. M. 2017, ARA&A, 55, 261

Katz, J. I. 2017, MNRAS, 471, L92
Katz, J. I. 2020, MNRAS, 494, L64
Kennicutt, R. C., Jr., Lee, J. C., Funes, J. G., et al. 2008, ApJS, 178, 247
Kirsten, F., Snelders, M. P., Jenkins, M., et al. 2021, Nat. Astron., 5, 414
Kirsten, F., Marcote, B., Nimmo, K., et al. 2022, Nature, 602, 585
Komatsu, E., Smith, K. M., Dunkley, J., et al. 2011, ApJS, 192, 18
Kovlakas, K., Zezas, A., Andrews, J. J., et al. 2020, MNRAS, 498, 4790
Kozlova, A. V., Israel, G. L., Svinkin, D. S., et al. 2016, MNRAS, 460, 2008
Kremer, K., Piro, A. L., & Li, D. 2021, ApJ, 917, L11
Kremer, K., Li, D., Lu, W., Piro, A. L., & Zhang, B. 2023, ApJ, 944, 6
Kuzmin, A. D. 2007, Ap&SS, 308, 563
Lemos, T., Gonçalves, R. S., Carvalho, J. C., & Alcaniz, J. S. 2023, Eur. Phys. J. C, 83, 138
Li, Y., Zhang, B., Nagamine, K., & Shi, J. 2019, ApJ, 884, L26
Li, C. K., Lin, L., Xiong, S. L., et al. 2021, Nat. Astron., 5, 378
Licquia, T. C., & Newman, J. A. 2015, ApJ, 806, 96
Lien, A. Y., Barthelmy, S. D., Baumgartner, W. H., et al. 2014, GRB Coordinates Network, 16522, 1
Liu, J.-F., Bregman, J. N., Bai, Y., Justham, S., & Crowther, P. 2013, Nature, 503, 500
Locatelli, N. T., Bernardi, G., Bianchi, G., et al. 2020, MNRAS, 494, 1229
Lorimer, D. R., Bailes, M., McLaughlin, M. A., Narkevic, D. J., & Crawford, F. 2007, Science, 318, 777
Lu, W., Beniamini, P., & Kumar, P. 2022, MNRAS, 510, 1867
Luo, R., Men, Y., Lee, K., et al. 2020, MNRAS, 494, 665
Maan, Y., Leeuwen, J. V., Straal, S., & Pastor-Marazuela, I. 2022, ATel, 15697, 1
Macquart, J. P., Prochaska, J. X., McQuinn, M., et al. 2020, Nature, 581, 391
Majid, W. A., Pearlman, A. B., Prince, T. A., et al. 2021, ApJ, 919, L6
Mannings, A. G., Fong, W.-F., Simha, S., et al. 2021, ApJ, 917, 75
Marcote, B., Paragi, Z., Hessels, J. W. T., et al. 2017, ApJ, 834, L8
Marcote, B., Nimmo, K., Hessels, J. W. T., et al. 2020, Nature, 577, 190
Margalit, B., Berger, E., & Metzger, B. D. 2019, ApJ, 886, 110
Margalit, B., Beniamini, P., Sridhar, N., & Metzger, B. D. 2020, ApJ, 899, L27
McConnachie, A. W., Irwin, M. J., Ferguson, A. M. N., et al. 2005, MNRAS, 356, 979
Mereghetti, S., Savchenko, V., Ferrigno, C., et al. 2020, ApJ, 898, L29
Newman, J. A., Ferrarese, L., Stetson, P. B., et al. 2001, ApJ, 553, 562
Niino, Y. 2020, ApJ, submitted [arXiv:2005.12891]
Nimmo, K., Hewitt, D. M., Hessels, J. W. T., et al. 2022, ApJ, 927, L3
Niu, C. H., Aggarwal, K., Li, D., et al. 2022, Nature, 606, 873
Olausen, S. A., & Kaspi, V. M. 2014, ApJS, 212, 6
Pastor-Marazuela, I., Connor, L., van Leeuwen, J., et al. 2021, Nature, 596, 505
Pearlman, A. B., & CHIME/FRB Collaboration 2022, ATel, 15792, 1
Petroff, E., Hessels, J. W. T., & Lorimer, D. R. 2019, A&ARv, 27, 4
Petroff, E., Hessels, J. W. T., & Lorimer, D. R. 2022, A&ARv, 30, 2
Pilia, M. 2021, Universe, 8, 9
Pilia, M., Burgay, M., Possenti, A., et al. 2020, ApJ, 896, L40
Pintore, F., Marelli, M., Salvaterra, R., et al. 2020, ApJ, 890, 166
Piro, L., Bruni, G., Troja, E., et al. 2021, A&A, 656, L15
Pleunis, Z., Good, D. C., Kaspi, V. M., et al. 2021, ApJ, 923, 1
Prochaska, J. X., Macquart, J.-P., McQuinn, M., et al. 2019, Science, 366, 231
Ptak, A., & Griffiths, R. 1999, ApJ, 517, L85
Rahmani, S., Lianou, S., & Barmby, P. 2016, MNRAS, 456, 4128
Rana, V., Harrison, F. A., Bachetti, M., et al. 2015, ApJ, 799, 121
Ransom, S. M., Eikenberry, S. S., & Middleditch, J. 2002, AJ, 124, 1788
Ravi, V., Catha, M., D'Addario, L., et al. 2019, Nature, 572, 352
Ravi, V., Law, C. J., Li, D., et al. 2022, MNRAS, 513, 982
Ravi, V., Catha, M., Chen, G., et al. 2023, ApJ, 949, L3
Rea, N., & Esposito, P. 2011, Astrophys. Space Sci. Proc., 21, 247
Ridnaia, A., Golenetskii, S., Aptekar, R., et al. 2020, GRB Coordinates Network, 27554, 1
Roberts, T. P., & Colbert, E. J. M. 2003, MNRAS, 341, L49
Ryder, S. D., Bannister, K. W., Bhandari, S., et al. 2022, arXiv e-prints [arXiv:2210.04680]
Schwab, J., Quataert, E., & Kasen, D. 2016, MNRAS, 463, 3461
Shappee, B. J., & Stanek, K. Z. 2011, ApJ, 733, 124
Sharma, K., Somalwar, J., Law, C., et al. 2023, arXiv e-prints [arXiv:2302.14782]
Sridhar, N., Metzger, B. D., Beniamini, P., et al. 2021, ApJ, 917, 13
Stamatikos, M., Malesani, D., Page, K. L., & Sakamoto, T. 2014, GRB Coordinates Network, 16520, 1
Stetson, P. B., Saha, A., Ferrarese, L., et al. 1998, ApJ, 508, 491
Tauris, T. M., Sanyal, D., Yoon, S. C., & Langer, N. 2013, A&A, 558, A39
Tavani, M., Verrecchia, F., Casentini, C., et al. 2020, ApJ, 893, L42
Tavani, M., Casentini, C., Ursi, A., et al. 2021, Nat. Astron., 5, 401
Tendulkar, S. P., Bassa, C. G., Cordes, J. M., et al. 2017, ApJ, 834, L7
Tendulkar, S. P., Gil de Paz, A., Kirichenko, A. Y., et al. 2021, ApJ, 908, L12
Thornton, D., Stappers, B., Bailes, M., et al. 2013, Science, 341, 53
Trudu, M., Pilia, M., Bernardi, G., et al. 2022, MNRAS, 513, 1858
Turolla, R., Zane, S., & Watts, A. L. 2015, Rep. Progr. Phys., 78, 116901
Wang, B., & Liu, D. 2020, RAA, 20, 135
Waxman, E. 2017, ApJ, 842, 34
Xu, J., & Han, J. L. 2015, RAA, 15, 1629
Yamasaki, S., & Totani, T. 2020, ApJ, 888, 105
Yao, J. M., Manchester, R. N., & Wang, N. 2017, ApJ, 835, 29
Younes, G., Kouveliotou, C., Jaodand, A., et al. 2017, ApJ, 847, 85
Zhang, C. F., Jiang, J. C., Men, Y. P., et al. 2020, ATel, 13699, 1
Zhong, S.-Q., & Dai, Z.-G. 2020, ApJ, 893, 9
Zhong, S.-Q., Xie, W.-J., Deng, C.-M., et al. 2022, ApJ, 926, 206